



**HAL**  
open science

## H Infinity robustification control of existing piezoelectric-stack actuated nanomanipulators

Hamid Ladjal, Jean-Luc Hanus, Antoine Ferreira

► **To cite this version:**

Hamid Ladjal, Jean-Luc Hanus, Antoine Ferreira. H Infinity robustification control of existing piezoelectric-stack actuated nanomanipulators. IEEE International Conference on Robotics and Automation ICRA2009, May 2009, Kobe, Japan. pp.3353 - 3358, 10.1109/ROBOT.2009.5152701 . hal-00657604

**HAL Id: hal-00657604**

**<https://hal.science/hal-00657604>**

Submitted on 7 Jan 2012

**HAL** is a multi-disciplinary open access archive for the deposit and dissemination of scientific research documents, whether they are published or not. The documents may come from teaching and research institutions in France or abroad, or from public or private research centers.

L'archive ouverte pluridisciplinaire **HAL**, est destinée au dépôt et à la diffusion de documents scientifiques de niveau recherche, publiés ou non, émanant des établissements d'enseignement et de recherche français ou étrangers, des laboratoires publics ou privés.

# $H_\infty$ Robustification Control of Existing Piezoelectric-Stack Actuated Nanomanipulators

Hamid Ladjal, Jean-Luc Hanus, Antoine Ferreira

**Abstract**—In current AFM-based nanomanipulation systems, the commercial position closed-loop controller for piezoelectric nanopositioning stages are implemented with success in a wide range of industrial applications. Even if these controllers operate with satisfactory nominal tracking performance, considerable attention has been focused on appropriate control strategies to compensate hysteresis, nonlinearities, drift and creep for high bandwidths and large scanning regimes. As these closed-loop controllers are very cost-effective, a special interest in robust plug-in compensators seems to be a solution. We proposed in this paper a robust plug-in compensator using the  $H_\infty$  loop-shaping techniques which can be plugged into the existing controller without affecting the already satisfactory nominal tracking performance of the existing closed-loop system. Dynamic modeling, identification and robust control of a 3 d.o.f. piezoelectric nanorobotic positioner are presented in this paper in order to improve the nanorobot performance under plant parameter variations and in the presence of external disturbances. Simulation and experimental results are given to validate the proposed plug-in robust compensator in the case of a nanorobotic manipulation task.

## I. INTRODUCTION

**I**N biotechnology field, the tele-nanomanipulation control of microobjects (biological cells, viruses, MEMS) with human handling is difficult due to dynamics and uncertainties which are strongly impacted by the user's gesture. In applications where high performance and accuracy are not critical constitutive nonlinearities of piezoelectric nanopositioning stages and hysteresis can be compensated by standard Proportional-Integral (PI) or Proportional-Integral-Derivative (PID) controllers, but this can potentially lead to bandwidth limitation and inefficiencies. Even if these controllers have proved their performance in nanoscale positioning systems, challenging problems of nanoscale control remain due to nonlinear dynamics, actuator's modeling uncertainties, instabilities and lack of robustness against external perturbations and sensor noise [1]. As these industrial closed-loop controllers are cost-effective and dedicated, a special interest in robust plug-in compensators seems to be a solution. The key idea of this paper is to robustify existing controllers by "Plug-In" attachable robust compensators for piezoelectric nanopositioning systems. Principle of the new methods is to settle on real plants as their nominal models with local compensators. Since the additional local compensators are designed independent of previously designed controllers, they are applicable for any existing control systems including nonlinear and/or non-closed form control scheme.

Hamid Ladjal is with PRISME Institute, ENSI de Bourges, F-18000 Bourges, France.

Antoine Ferreira is with PRISME Institute, ENSI de Bourges, F-18000 Bourges, France (e.mail: antoine.ferreira@ensi-bourges.fr).

A brief analysis of robust control techniques shows that a considerable number of feedback design schemes based on linear robust control techniques have been already proposed for nanopositioning systems. Development of inversion-based feedforward control with robust feedback control have proved their efficacy in output tracking in Atomic Force Microscope [2], [3]. The performance of the inverse feedforward control, however, is strongly limited by modeling errors/uncertainties and disturbances [4]. Closed-loop linear  $H_\infty$  control technique seems to be an efficient alternative technique. These schemes have provided improvements in bandwidth and robustness to non linearities and hysteresis. In [5], the authors proposed a Smith predictor-based  $H_\infty$  controller for a piezoactuator with an emphasis in reducing the hysteresis. In [6], a  $H_\infty$  controller design for one-dimensional nanopositioning system performing high closed-loop bandwidths and robustness against nonlinearities has been synthesized with success. Finally, a robust Glover-McFarlane  $H_\infty$  scheme [7] to simultaneously achieve performance and robustness where neither specific tracking requirement nor a characterization of uncertainty are available *a priori*.

Considering these robust control schemes, we proposed a framework for increasing the robustness of existing industrial control schemes with a quantifiable compromise on performances. We proposed in this paper a robust plug-in compensator using the  $H_\infty$  loop-shaping techniques which can be plugged into the existing controller without affecting the already satisfactory nominal tracking performance of the existing closed-loop system. A similar approach has been introduced by Salapaka in [8]. In the present study, the  $H_\infty$  loop-shaping technique is applied for robustification of complex industrial controllers achieving robustness with marginal reduction in performance. Dynamic modeling, identification and robust control of a 3 degree of freedom piezoelectric nanorobotic positioner are presented in this paper in order to improve the nanorobot performance under plant parameter variations and in the presence of external disturbances.

The paper is organized in the following way. In Section 2, a description of the nanorobotic device is given. This is followed by the frequency-domain-based system identification of the existing controller and nanorobotic positioner. The control design and the experimental results are then presented in Section 4. Experimental results are given in Section 5 to validate the proposed plug-in robust compensator in the case of a nanorobotic manipulation task.

## II. PIEZOELECTRIC NANOMANIPULATOR DESCRIPTION

The nanomanipulator structure is composed of three linear translation stages (x,y,z) driven by DC motors for coarse

motion (range: 8 mm, accuracy: 15 nm) combined with a 3 d.o.f ultra-high-resolution piezomanipulator ( $x,y,z$ ) for fine positioning (range: 100  $\mu\text{m}$ , accuracy: 1 nm). This hybrid nanomanipulation system combines the advantages of ultra-low inertia, high-speed and long travel range (Fig.1(a)). The micro-endeffector is constituted by a piezoresistive AFM cantilever integrating a full-bridge strain gauge sensors ((Fig.1(b)).

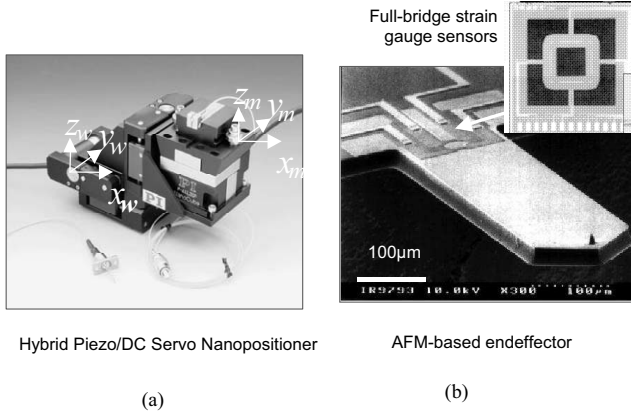


Fig. 1. Structure of the hybrid 6 dof AFM-based nanomanipulator and its sensorized force cantilever.

The 3 d.o.f ultra-high-resolution piezomanipulator (P-611.3S NanoCube from Physics Instruments) is a versatile, multi-axis piezo-nanopositioning system. Its 100 x 100 x 100  $\mu\text{m}$  positioning and scanning range comes in an extremely compact package. Equipped with a zero-stiction, zero-friction guiding system, this piezomanipulator provides motion with ultra-high resolution and settling times of only a few milliseconds. Single-axis nanopositioning stage with anti-accurate-motion flexure design. The best flexure designs provide guiding precision in the low nanometer range. In open-loop operation, the platform's position is roughly proportional to the drive voltage. In the closed-loop version, the Proportional-Integral controller allows absolute position control. However, existing closed-loop controller is designed to achieve specific tracking and performance requirements (such as zero steady-state tracking) in a narrow frequency closed-loop bandwidth. During nanomanipulation tasks, the x-y-z nanopositioner servo-controller lacks in robustness against:

- a) Modeling uncertainties:
  - 1) Mechanical nonlinearities of mechanical-guiding systems for large travel ranges;
  - 2) Modeling uncertainties due to operating point, temperature effects and time execution;
  - 3) Hysteresis and creep effects due to piezoelectric ceramics.
- b) External perturbations:
  - 1) Noise measurement perturbations;
  - 2) Force/torque perturbations during nanomanipulation.

Considering these limitations, we proposed in the following a robust plug-in compensator using the  $H_\infty$  loop-shaping technique which can be plugged into the existing PI-controller without affecting the already satisfactory nominal tracking performance.

### III. CONTROLLER DESIGN AND IDENTIFICATION

#### A. Controller Design

In this paper, we simply assume that the controller has been already designed by the manufacturer and is in operation in a real micromanipulation system. However, it is often the case that this controller may not work well when the plant is perturbed and/or external disturbances presents. In this situation, an additional controller is needed to improve the robustness of the overall system against plant uncertainties. It is desirable that this additional controller can be plugged into the existing controller and without affecting the already satisfactory tracking performance. Considering these limitations, we proposed in the following a robust plug-in compensator using the  $H_\infty$  loop-shaping technique which can be plugged into the existing PI-controller without affecting the already satisfactory nominal tracking. This the reason why we called that controller a plug-in controller.

#### B. Identification

The digital system to be identified is constituted of both components: the piezoelectric nanopositioner and the PI-controller embedded into the acquisition card. The acquisition board is composed of digital inputs (DAC) and outputs (ADC), the identification should be considered as a discrete system. Among the various modes of identification for numerical systems ([9], [10]), we choose the least squares simple method. This choice is justified by the simplicity of the method during implementation, accuracy of the identified parameters and off-line parameters adjustment. The least square method is based on the determination of a vector of parameters so as to minimize a error vector  $\varepsilon$ :

$$J(\vartheta) = \|\varepsilon(k)\|^2 = (y(k) - \phi(k)\vartheta)^T (y(k) - \phi(k)\vartheta) \quad (1)$$

The vector parameters minimizing the criterion  $J(\vartheta)$ , denoted  $\hat{\vartheta}(k)$ , is called the estimated vector parameters defined by ([10]):

$$\hat{\vartheta}(k) = (\phi^T(k)\phi(k))^{-1}\phi^T(k)y(k) \quad (2)$$

where  $\phi(k)$  is the observation matrix  $\phi(k)$  of  $p$ -order. In to order to identify the wide dynamics bandwidth of the servo-nanopositioner, we chose a Pseudo-Random Pattern Generator signal (PRPG). It has been already proved reliable for a good identification in many dynamic systems. The scheme of Fig.2 depicts the principle of the numerical identification.  $U(Z)$  represents the numerical input signal (PRPG input signal),  $Y(Z)$  the numerical output signal of the system. The system is provided with analog-to-digital and digital-to-analog converters which make it possible to pass from discrete towards the continuous and the continuous towards the discrete space.

In Fig.2, the terms  $G(S)$  and  $H(z)$  represent the transfer functions of the continuous system and the discrete system, respectively. The parameters provided by the identification represent the  $a_i$  and the  $b_j$  of the discrete transfer function which is given by the following expression:

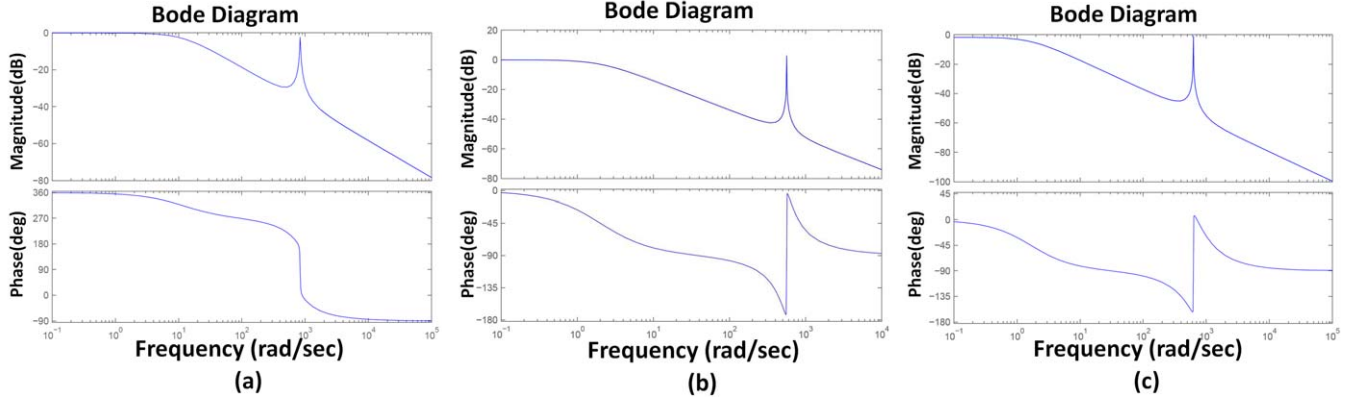


Fig. 3. Experimental frequency responses of (a) x-axis, (b) y-axis and (c) z-axis.

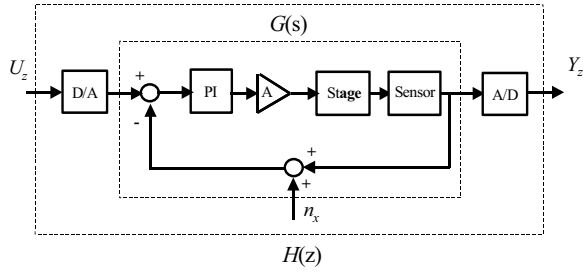


Fig. 2. Identification system of the transfer function.

$$\frac{b_0z^2 + b_1z + b_2}{z^3 + a_1z^2 + a_2z + a_3} \quad (3)$$

The identification was carried out for several operating points, ranging from 0 to  $60\mu\text{m}$  with elementary steps of  $10\mu\text{m}$  order and driving frequencies lower than the resonance frequencies. The discrete models have been identified with averaged parameter values for  $x$ ,  $y$  and  $z$  axes, respectively

$$H_x(z) = \frac{0.00535z^2 + 0.0271z + 0.0507}{z^3 - 0.00557z^2 + 0.0196z - 0.93} \quad (4)$$

$$H_y(z) = \frac{0.003z^2 + 0.00741z + 0.0117}{z^3 - 0.00579z^2 + 0.025z - 0.997} \quad (5)$$

$$H_z(z) = \frac{0.000556z^2 + 0.00535z + 0.00761}{z^3 - 0.00566z^2 + 0.0222z - 1} \quad (6)$$

Then, we used the Matlab function *d2c* to convert the discrete functions to continuous functions. The results presented in Fig.3 show the experimental frequency responses. These results show good tracking performances with negligible error. However, it should be noticed that the identified models vary strongly due to uncertain dynamics and are subject to modeling uncertainties.

#### IV. PLUG-IN ROBUST CONTROLLER DESIGN

The existing controller is a proportional integral (PI) and for the robustification of the existing controller we use the  $H_\infty$  loop shaping technique and how it can be integrated in a robust plug-in controller.

##### A. Coprime Factorization Approach

An approach was developed by ([11]) and ([12]) starting from the concept of the coprime factorization of transfer matrix. This approach presents interesting properties and its implementation calls upon notions traditional of automatic control.

##### B. Robust Controller Design using Normalized Coprime Factor

We define the nominal model of the system to be controlled starting from the coprime factors on the left:  $G(s) = \tilde{M}(s)^{-1}\tilde{N}(s)$ . Then a perturbed model is written (see Fig .4).

$$\tilde{G} = (\tilde{M} + \Delta_m)^{-1}(\tilde{N} + \Delta_n) \quad (7)$$

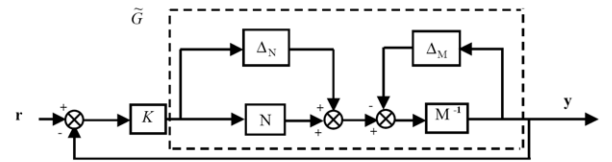


Fig. 4. Coprime factor robust stabilization problem.

where  $\tilde{G}$  is a left coprime factorization (LCF) of  $G$ , and  $\Delta_m, \Delta_n$  are unknown and stable transfer functions representing the uncertainty. We can then define a family of models with the following expression :

$$\xi_\varepsilon = \{\tilde{G} = (\tilde{M} + \Delta_m)^{-1}(\tilde{N} + \Delta_n) : \|(\Delta_m \ \Delta_n)\|_\infty < \varepsilon\} \quad (8)$$

where  $\varepsilon_{max}$  represent the margin of maximum stability. The robust problem of stability is thus to find the greatest value

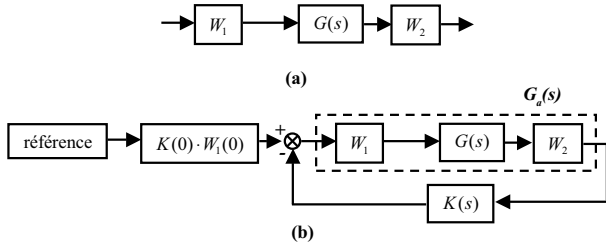


Fig. 5. Loop Shaping design procedure.

of  $\varepsilon = \varepsilon_{max}$ , such as all the models belonging to  $\xi_\varepsilon$  can be stabilized by the same corrector  $K$ . The problem of robust stability  $H_\infty$  amounts finding  $\gamma_{min}$  and  $K(s)$  stabilizing  $G(s)$  such as:

$$\left\| \begin{pmatrix} I \\ K \end{pmatrix} (I - GK)^{-1} \begin{pmatrix} I & W_2 G W_1 \end{pmatrix} \right\|_\infty = \gamma_{min}^{-1} = \varepsilon_{max}^{-1} \quad (9)$$

However, [13] showed that the minimal value  $\gamma$  of is given by:

$$\gamma_{min} = \varepsilon_{max}^{-1} = \sqrt{1 + \lambda_{sup}(XY)} \quad (10)$$

where  $\lambda_{sup}$  indicates the greatest eigenvalue of  $XY$ . Moreover, for any value  $\varepsilon < \varepsilon_{max}$  a corrector stabilizing all the models belonging to  $\xi_\varepsilon$  is given by:

$$\begin{aligned} K(s) &= B^T X (sI - A + BB^T X - \gamma^2 Z Y C^T C)^{-1} \gamma^2 Z Y C^T \\ Z &= (I + YX - \gamma^2 I)^{-1} \\ \gamma &= \varepsilon^{-1} \end{aligned} \quad (11)$$

where  $A$ ,  $B$  and  $C$  are state matrices of the system defined by the function  $G$  and  $X$ ,  $Y$  are the positive definite matrices and solution of the Ricatti equation.

### C. The Loop Shaping Design Procedure

Contrary to the approach of Glover-Doyle, no weight function can be introduced into the problem. The adjustment of the performances is obtained by affecting an open modeling (*Loop Shaping*) process before calculating the compensator. The design procedure is as follows :

- We add to the matrix  $G(s)$  of the system to be controlled a pre-compensator  $W_1$  and/or a post-compensator  $W_2$ . The nominal plant  $G(s)$  and shaping functions  $W_1$  and  $W_2$  are combined in order to improve the performances of the system such as  $G_a(s) = W_2(s)G(s)W_1(s)$  (see Fig.5.a).
- From coprime factorizations of  $G_a(s)$ , we apply the previous results to calculate  $\varepsilon_{max}$ , and then synthesize a stabilizing controller  $K$  ensuring a value of  $\varepsilon$  slightly lower than  $\varepsilon_{max}$ .
- The final feedback controller is obtained by combining the  $H_\infty$  controller  $K$  with the shaping functions  $W_1$  and  $W_2$  such that  $G_a(s) = W_2(s)G(s)W_1(s)$  (See Fig.5.b).

## V. CHARACTERIZATION OF PIEZOELECTRIC-STACK ACTUATED NANOMANIPULATOR

### A. Implementation of the controllers

The controller  $K$  is obtained by combining the pre-filter and the post-filter . The pre-filter and post-filter are used to shape the open-loop plant to achieve a desired frequency responses according to some well defined design specifications such as bandwidth and steady-state error ([15]). To obtain a high gain at low frequency, a *PI* controller is synthesized for the x-axis like pre-filter  $W_1$  and in order to obtain a small gain at high frequency, a low-pass filter is synthesized like pre-filter  $W_2$ . In order to obtain a high performance and a good robustness, we add the following weight functions:

$$W_1 = 50 \times \frac{10s+35.2}{10s}, W_2 = \frac{1}{s+11.3}.$$

Using this weight functions we obtain six-order the  $H_\infty$  controller. In order to implement this controller we use the function of Matlab *balmr* to reduce the order and obtain a third-order approximation of the plug-in robust controller given by :

$$K_r(s) = \frac{-72.69s^2 - 1824s - 6706}{s^3 + 66.88s^2 + 625.7s - 5.07 \times 10^{-11}}. \quad (12)$$

and the discrete controller :

$$K_{rd}(s) = \frac{0.1726z^2 - 0.3347z + 0.1622}{z^3 - 2.842z^2 + 2.688z - 0.846} \quad (13)$$

The Fig. 6 and Fig. 7 show the frequency responses of the weight functions  $W_1$ ,  $W_2$ , of the open-loop system  $W_1.P.W_2$  and of the controller  $K$ . The results show that the open-loop remains close to the step response obtained after the choice of the shaping functions and  $K_r$  ensures correct margins of stability.

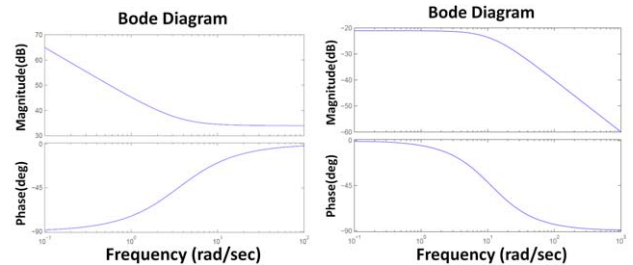


Fig. 6. Bode diagram of  $W_1$  and  $W_2$ .

### B. Nanomanipulator Characterization

In this section, the nanopositioning is characterized in terms of range, sensitivity and resolution in the open- and closed-loop configurations. The calibration data showed some hysteresis in open-loop. Hysteresis is primarily due to the nonlinear relationship between applied voltage and displacement which are important for large deflections. To present the effectiveness of the  $H_\infty$  closed-loop design, the hysteresis

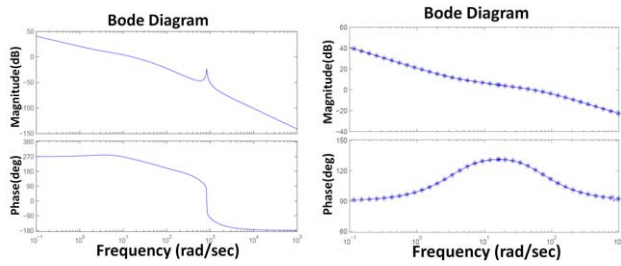


Fig. 7. Bode diagram of open-loop system  $W_1.P.W_2$  and  $K_r$ .

curves obtained in open-loop are compared with the closed-loop design using  $PI$  controller and the  $H_\infty$  controller. We can see clearly that for a nanopositioning displacement of  $40\mu m$ , a maximum output hysteresis of  $10\mu m$  (25%) was observed. The same experiment with the closed-loop controller showed that the effects were practically eliminated (Fig.9). An important observation comes from the fact that the operating applied voltage is settled to 100V while the system was identified for a low value of input signal (PRPG signal). It shows clearly the linearity relationship between the input-output signals. Similar linearity results have been measured when considering creep effects. It should be noticed that important differences were observed for different displacement with  $PI$  and  $H_\infty$  controller. High precision is obtained with robustified  $PI$  controller.

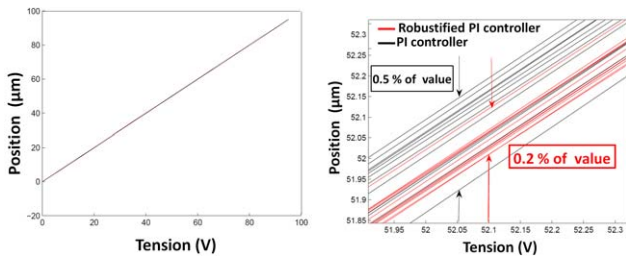


Fig. 9.  $PI$  and  $H_\infty$  controller to remove the hysteresis and the zoom of the response.

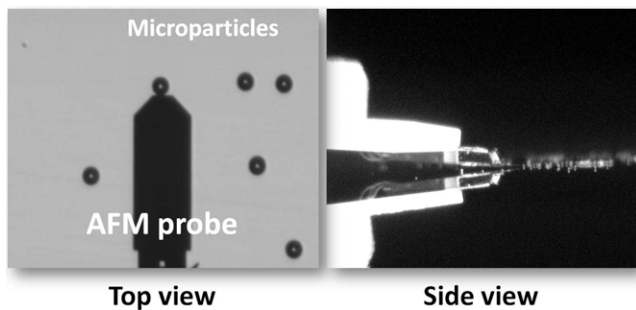


Fig. 10. Different optical microscope views (top view, side view and zoom view) of the nanomanipulator pushing microparticles of  $5\mu m$  of diameter.

### C. Robust Experimentation in Microsphere pushing

To illustrate the behavior of the piezoelectric-stack actuated nanomanipulator system and to confirm the findings of the previous section. The working space of the nanomanipulator

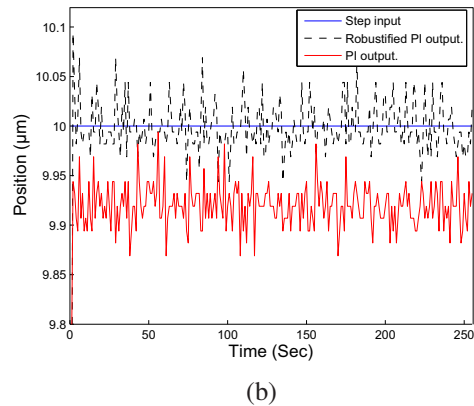
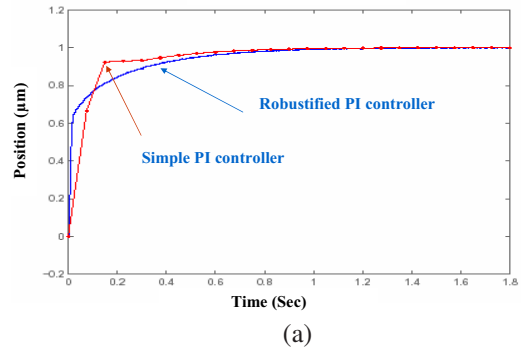


Fig. 11. (a) Step responses for  $PI$  and  $H_\infty$  controllers and (b) corresponding static errors.

is visualized through two orthogonal optical microscopes (top-view and side-view) and a high magnification microscope for a zooming view (see Fig.10). The micromanipulation task is to realize micro pushing tasks of microparticles of  $5\mu m$  of diameter on a glass substrate. During the micro pushing tasks, we made a comparison between the responses with  $PI$  and  $H_\infty$  controllers when pushing a microparticle. We give different responses of the system with plug-in robust controller in the presence of the disturbance and position sensor noise. The set of experiments of Fig.11 shows the position with the plug-in robust controller. The experimental results demonstrate the excellent position tracking with the proposed plug-in robust controller and the output track the reference and we can see clearly the better tracking  $PI$  controller (Fig.11.b). The experimental response with a step perturbation demonstrate the excellent tracking and the position follows well the reference and not affected by the application of a disturbance (Fig.12.a). To emphasize the noise problem of the closed loop system with the plug-in robust, Fig.12.b demonstrate the influence of this parameter on the performance of the robust controller. Fig.12.b show clearly a better tracking of position variable with significant noise sensor.

## VI. CONCLUSION

The Loop Shaping Design Procedure using  $H_\infty$  synthesis has been applied for robustified controller design of piezoelectric-stack actuated nanomanipulators. In the proposed  $H_\infty$  loop shaping design procedure, the model uncertainties are included

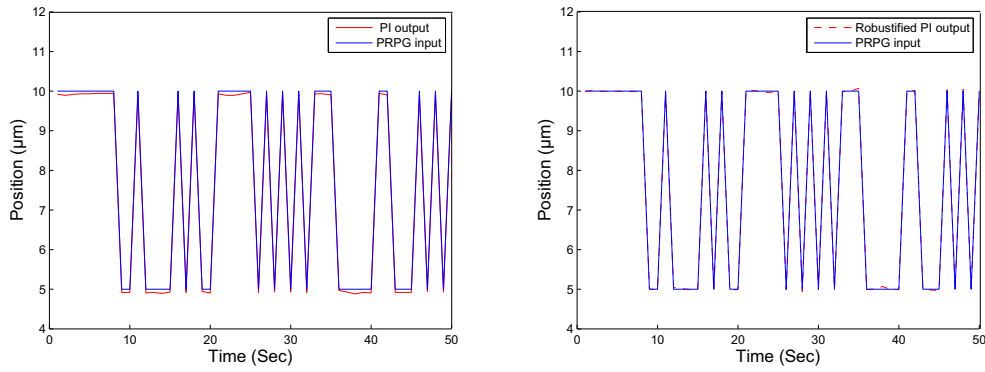


Fig. 8. PRPG responses with (a) *PI* controller (b) robustified *PI* controller.

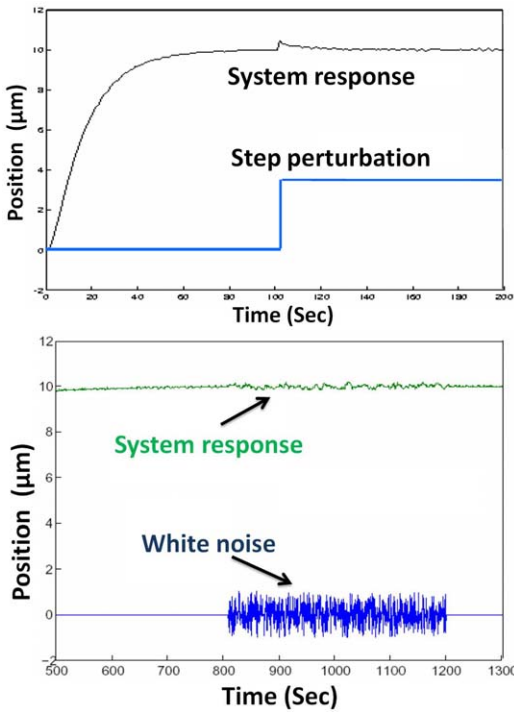


Fig. 12. Step responses with robustified *PI* controller in presence of (a) step perturbation (b) white noise.

as perturbations to the nominal model, and robustness is guaranteed by ensuring that the stability specifications (nanometer resolution) are satisfied in the worst-case uncertainty. As conclusion, a very good point of the design is the remarkable features that achieves robustness with marginal reduction of performance. Our future work will consist of using the piezoelectric-stack actuated nanomanipulators in robust nanoteleoperation of mouse embryonic stems cells (mESC)s for regenerative cell construction.

## REFERENCES

[1] P. Ge, M. Jouaneh, "Tracking control of a piezoceramic actuator" *IEEE Transactions on Control Systems Technology*, Vol.4, No.3, pp. 209–216, May.1996.  
 [2] Q. Zou, K.K. Leang, E. Sadoun, M.J.Reed, S. Devasia, "Control issues in high-speed AFM for biological applications: Collagen imaging example", *Asian Journal Control*, Vol.8, pp.164–178, Jun.2004.

[3] Q. Zou, S. Devasia, "Preview-based optimal inversion for output tracking: Application to scanning tunneling microscopy". *IEEE Transactions on Control Systems Technology*, Vol.12, pp. 375–386, May.2004.  
 [4] S. Devasia, "Should model-based inverse input be used as feedforward under plant uncertainty", *IEEE Transactions on Automatic Control*, Vol.47, pp. 1865–1871, Nov.2002.  
 [5] M. Tsai, J. Chen, "Robust Tracking control of a piezoactuator using a new approximative hysteresis model", *Journal of Dynamics Systems, Measurement and Control*, Vol.125, pp. 96–102, Mar.2003.  
 [6] S. Salapaka, A. Sebastian, J. P. Cleveland, V. Salapaka, "High bandwidth nano-positioner: a robust control approach", *Review of Scientific Instruments*, Vol.73, No.9, pp.3232–3241 Sep.2002.  
 [7] A. Sebastian, S. M. Salapaka, " $H_\infty$  loop shaping design for nanopositioning", *American Control Conference*, Denver, CO, Jun.2003, pp. 3708–3713.  
 [8] A. Sebastian, S. M. Salapaka, "Design Methodologies for Robust Nano-Positioning", *IEEE Transactions on Control Systems Technology*, Vol.13, No.6, pp. 868–876, Nov.2005.  
 [9] R. Longchamp, "Commande numérique de systèmes dynamiques", *Presse polytechnique*, Lausanne 2006.  
 [10] M. Rivoire, J.-L. Ferrier, Cours d'automatique Tome 3, "Commande par ordinateur", 1992.  
 [11] K. Glover, D. Mc Farlane, "Robust stabilization of normalized coprime factors: An explicit  $H_\infty$  solution", *IEEE American Control Conference*, Atlanta, GA, 1988.  
 [12] K. Glover, D. Mc Farlane, "Robust Stabilization of normalized coprime factor plant descriptions with  $H_\infty$  bounded uncertainty", *IEEE Transactions on Automatic Control*, Vol. 34, pp. 821–830, 1989.  
 [13] D. Mc Farlane, K. Glover, "A Loop Shaping design procedure using  $H_\infty$  synthesis", *IEEE Transactions on Automatic Control*, Vol 37, pp.759–769, 1992.  
 [14] G.J. Balas, J.C. Doyle, K. Glover, A. Packard, and R. Smith, " $\mu$ -Analysis and Synthesis Toolbox", Natick, MA: *The MathWorks*, Inc, 1994.  
 [15] P. Lundstrom, S. Skogstad, Z.C. Wang, "Weight selection for  $H_\infty$  and  $\mu$ -control methods: insights and examples from process control", *Workshop on  $H_\infty$  Control*, Brighton, U.K., pp.139–1991, 1991.